RESEARCH PAPER

A Model Based Analysis of IPEC Dosing of Paclitaxel in Rats

Pieter Colin • Lieselotte De Smet • Chris Vervaet • Jean-Paul Remon • Wim Ceelen • Jan Van Bocxlaer • Koen Boussery • An Vermeulen

ABSTRACT

Purpose A strong pharmacokinetic rational exists for the use of (Hyperthermic) Intraperitoneal Perioperative Chemotherapy in peritoneal carcinomatosis. However, controversy remains regarding the optimal treatment strategies. Paclitaxel is believed to be a good compound for IPEC treatment because of its favourable pharmacokinetic properties.

Methods Rat experiments were set up to gain insight in PTX's pharmacokinetics and pharmacodynamics after IPEC treatment with Taxol®. Afterwards a Pharmacokinetic—Pharmacodynamic model was developed, that concurrently describes plasma and tumour exposure post IPEC dosing. Moreover, the developed model adequately describes the time-course of tumour apoptosis as well as the treatment effect on tumour volume.

Results We show that the complex absorption processes underlying PTX absorption from the peritoneal cavity post IPEC dosing, give rise to a markedly non-linear dose response relationship. Furthermore, we show that, in order to optimize treatment efficiency whilst concurrently minimizing the possibility of systemic toxicities, lowering the dose and extending exposure to the cytotoxic solution is the way forward.

Conclusions Based on the close resemblance between tumour exposure in our animal model and tumour exposure in patients treated under similar conditions, we hypothesise that, according to our findings in the rat, in the treatment of PC using IPEC administration of PTX, less is truly more.

P. Colin (✉) • J. Van Bocxlaer • K. Boussery • A. Vermeulen
Laboratory of Medical Biochemistry and Clinical Analysis, Faculty of
Pharmaceutical Sciences, Ghent University, Ghent, Belgium
e-mail: Pieter.Colin@ugent.be

L. De Smet • C. Vervaet • J.-P. Remon
Laboratory of Pharmaceutical Technology, Faculty of Pharmaceutical
Sciences, Ghent University, Ghent Belgium

INTRODUCTION

Since its first description in 1980 by Spratt *et al.* (1), hyperthermic intraperitoneal perioperative chemotherapy (HIPEC) has gained interest as an alternative treatment option to systemically administered chemotherapy for the treatment of peritoneal carcinomatosis (PC). During hyper-/normothermic IPEC, a solution containing a cytotoxic agent is instilled into the peritoneal cavity for 30–120 min (2). During the treatment, an external heater circulator is used to maintain the temperature of the solution at mild hyperthermic (41–43°C) or normothermic (37°C) conditions.

During surgery, the abdominal muscle wall is expanded using traction sutures on the skin, thereby elevating the skin's edge,

W. Ceelen
Laboratory of Experimental Surgery, Ghent University Hospital, Ghent
Belgium

creating a pouch to contain the cytotoxic solution. This technique, known as the "open" technique, which allows the surgeon to manipulate the abdominal contents during the procedure, thereby homogeneously distributing the cytotoxic solution throughout the patient's abdomen, is usually preferred. After 30–120 min, the remaining solution is removed from the peritoneal cavity and the patient's abdominal wall is sutured.

In the treatment of cancers confined to the peritoneal cavity (e.g., PC), Dedrick *et al.* (3) hypothesized that this type of regional treatment could increase treatment efficiency by exposing tumours within the peritoneal cavity to higher drug concentrations. Furthermore, the peritoneal-plasma barrier is thought to limit/slow drug clearance from the peritoneal cavity to the systemic circulation, thereby minimizing systemic exposure and systemic adverse effects.

Although IPEC as a tool for regional drug delivery has a strong pharmacokinetic rationale, controversy remains regarding the optimal treatment strategies that will optimize efficacy whilst minimizing systemic exposure (4). Besides the ongoing debate on the additional benefit of hyperthermia in IPEC, questions regarding the dose to be administered, the duration of the perfusion or the optimal carrier solution to be used hamper the routine implementation of IPEC (5).

Paclitaxel (PTX) is believed to be a good compound for IPEC treatment because of its favourable pharmacokinetic properties. Its high molecular weight is hypothesized to slow down clearance from the peritoneal cavity (4) into the bloodstream, thereby maximizing contact time with the peritoneal tumours. Furthermore, its high systemic clearance, as well as its pronounced first-pass effect are believed to limit systemic exposure after IPEC treatment. Although these pharmacokinetic advantages favour the use of PTX in IPEC, the limited knowledge on the degree of tumour penetration and accumulation along with the aforementioned issues regarding IPEC administration, currently limit its use in clinical centres.

This study was set up to gain insight in PTX's pharmacokinetics (PK) and pharmacodynamics (PD) after IPEC treatment using Taxol® in a rat model for PC. Concurrently, we investigated the influence of the treatment modalities (i.e. the effect of dose and duration of perfusion) on treatment outcome. In addition, the degree of PTX penetration in tumour tissue was quantitatively determined and linked to observed pharmacological effects after IPEC treatment in an *in-vivo* rat model for PC.

MATERIALS AND METHODS

Experimental Procedures

Materials

Taxol® (6 mg/ml PTX in a 1:1 Cremophor®EL/ethanol mixture) from Bristol-Myers Squibb (Brussels, Belgium) was weighted and dissolved in 125 mL of a 0.9% NaCl solution to obtain the solutions (0.24 mg/mL or 0.024 mg/mL) for IPEC treatment. These concentrations were chosen based on previous (unpublished) work that determined 0.24 mg/mL as the maximum tolerable dose following IPEC administration for 45 min.

Rat Tumour Model

A human ovarian carcinoma cell line (SKOV-3, obtained from the American Type Culture Collection) was cultured at 37°C in a 5% CO_2-containing humidified atmosphere. SKOV-3 cells were cultured in McCoys medium (Invitrogen, Merelbeke, Belgium), which was supplemented with 10% fetal bovine serum, penicillin, streptomycin (Invitrogen, Merelbeke, Belgium) and fungizone (Bristol Myers Squibb, Brussels, Belgium).

Adult female athymic nude rats (Harlan, Horst, The Netherlands) were kept in standard housing conditions with water and food *ad libitum* and a 12 h light/dark circle. All animal experiments were approved by the local ethics committee.

Donor rats were injected with 30×10^6 SKOV-3 cells in a volume of 0.2 ml between the peritoneum and the abdominal muscle to induce tumour formation. The animals received a daily subcutaneous administration of 3 mg cyclosporine from 3 days prior until 10 days after injection of the SKOV-3 cells. After 3 to 4 weeks, tumours had sufficiently grown to transplant tumour samples (5×5 mm, with a thickness of 3 mm) on the parietal peritoneum of another acceptor rat. The acceptor rat was dosed with cyclosporine in the same way as the donor rat. Approximately 3 weeks after transplantation, tumours had grown sufficiently to perform IPEC.

IPEC Procedure

After anesthetizing each rat with 3% isoflurane (Forene®, Abbott, Waver, Belgium), a vertical incision in the abdominal wall muscle was made along the midline. The abdominal wall muscle was attached to a metal ring which was placed a few centimeters above the incision. The inlet and outlet tubing (Pumpsil®, Watson-Marlow, Zwijnaarde, Belgium) was placed in the peritoneal cavity for perfusion with the cytostatic solution. A roller pump (Watson-Marlow, Zwijnaarde, Belgium) circulated the cytostatic solution through a heat exchanger set at 37°C. During perfusion, the perfusate solution and body temperature of the rat were closely monitored. When the perfusion was finished, the peritoneal cavity was flushed with 0.9% NaCl solution and the abdominal wall was sutured.
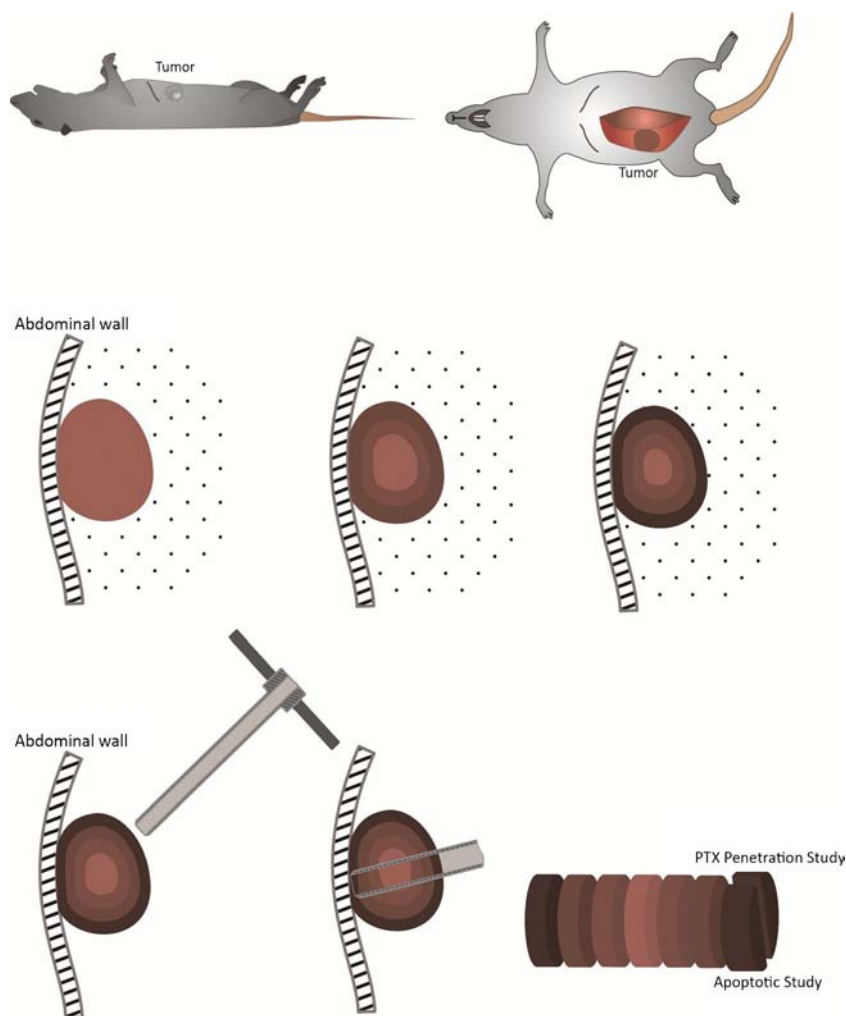
Tumour Collection

Tumours were excised at different time points (5, 15, 30, 45, 60, 90, 120, 240 and 480 min) after starting IPEC treatment. After excision of the tumour, rats were euthanized. A cross-section of the tumour was cut out, perpendicular to the peritoneal membrane, to obtain a cylinder-shaped tumour sample (±10 mm of diameter) (Fig. 1). This cylinder was split in half. After further sub-sectioning, one half was frozen at −20°C for PTX concentration determinations whilst the other half was formalin-fixed and paraffin-embedded for caspase-9 staining.

Collection of Plasma and Perfusate Samples

Blood was sampled in heparin-containing tubes via a catheter that was placed in the arteria carotis or arteria femoralis. Blood samples were taken between 5 min and 8 h after starting the perfusion. Blood samples were immediately centrifuged at 2000 g at room temperature, and separated plasma was stored at −80°C until analysis.

During a pilot study, samples were collected from the perfusion solution used during the IPEC administration.

Samples were collected at the start of the IPEC procedure and 15, 30 and 45 min thereafter.

Plasma and perfusate samples were analysed as described previously (6).

Tumour Tissue Concentration Measurements

After rinsing and weighing of the tumour section, a tumour tissue aliquot, weighing exactly 25 mg, was suspended in water and mechanically disrupted. Subsequently, internal standard (^{13}C-paclitaxel) was added. Tumour tissue was then enzymatically digested using a proteinase-K and a lipase solution (both Sigma-Aldrich, Belgium). Tissue suspensions were left to incubate overnight at 55°C whilst continuously being shaken.

After centrifugation of the digested tissue suspension at 10,000 g for 20 min, supernatant was collected and subjected to solid phase extraction. In short, after loading of the sample, the SPE cartridges (Oasis® HLC cartridges, Waters, USA) were washed with a sodium hydroxide (pH 10.0) solution and eluted using a 70% (v/v) methanol solution in water. Following elution, samples were concentrated by evaporation of methanol under a mild nitrogen stream (30 min, 35°C).

Fig. 1 Tumour harvesting protocol.

Finally, after reconstitution, samples were injected onto the Waters Acquity UPLC system (BEH C18 column). Paclitaxel and ^{13}C-paclitaxel were detected with a Quattro Ultima triple quadrupole system (Micromass Waters, Manchester, UK). The measurement range of the analytical method was 0.035–8.3 µg/g. Total imprecision and bias were calculated based on results of repeated analysis of quality controls (QC) and analysis values were reported only if quantification of the QC samples complied with the FDA guidance specifications on maximum tolerable bias and imprecision [7] (trueness <15% and total imprecision <15%) (Analytical paper submitted to *Talanta*).

Apoptosis Measurements

After sample preparation, using xylene and ethanol, to remove a.o. the paraffin layer, tumour sections, 5 µm thick, were obtained through a rotary microtome (HM® 360, Microm, Walldorf, Germany). After washing in physiologically buffered saline (PBS), heat-induced antigen retrieval was performed for 30 min in a citrate buffer (pH 6.0), after which the tissue slices were cooled down for 15 min at room temperature. The endogenous peroxidase activity was blocked for 15 min with a 0.3% hydrogen peroxide solution (DAKO, Glostrup, Denmark). After the washing steps, each section was treated with a blocking solution (Tris-Buffered saline 0.1%) for 1 h at room temperature. Primary antibody Cleaved caspase-9 (Cell signaling Technology, Leiden, The Netherlands, 1/400 in PBST 5%) was incubated overnight at 4°C. After washing, the tissue sections were incubated for 30 min at room temperature with a labelled polymer horse-radish peroxidase anti-rabbit secondary antibody (DAKO). A colour was developed using the chromogen 3,3-diaminobenzidine+ (DAB) for 10 min. After washing, the tissue sections were counterstained with Mayer's haematoxylin for 2 min.

The number of apoptotic cell fragments present in each tissue section was expressed as a fraction of the total number of cells. The apoptotic index was determined with an Optronics Color digital camera (Olympus Corporation, Tokyo, Japan) and specialized software (Cell D Olympus Imaging Solutions, Münster, Germany). Ten regions of interest (ROI) were chosen at random at a magnification of 200×. The final apoptotic index used in the data-analysis was the geometric mean of these 10 ROI. Highly necrotic regions were excluded from the analysis.

Tumour Volume Measurements

Tumour growth was evaluated via a Siemens® Trio 3 T clinical MRI scanner (Erlangen, Germany). Prior to the MRI scan, rats were anaesthetized with Rompun 2% (Bayer, Diegem, Belgium) and ketamine (Ceva, Amersham, UK) using a dose of 10 mg/kg and 90 mg/kg, respectively.

The rats were placed prone in a (wrist) coil to measure the tumour volume. A T1-weighted 3D FLASH sequence was applied with a flip angle of 10°, a repetition time of 13 ms and an echo time of 4.9 ms to obtain a voxel size of $0.19 \times 0.19 \times 0.4$ mm^3. Tumour volume was defined by creating a volume of interest (VOI) consisting of a stack of planar regions of interest (ROI) using PMOD software (PMOD Technologies, Adliswil, Switzerland). Rats were scanned 1 day prior to IPEC treatment to measure the initial volume of the tumour. Subsequently, tumour volume was evaluated 7 and 14 days after IPEC treatment.

Available Data

The final dataset consists of data collected throughout different study periods (no previously published data were used). In one of the studies, 3 rats were used to evaluate the PK behaviour of PTX in absence of other Taxol® excipients. Therefore, in these rats, 105 µg of PTX was administered intravenously by fortifying 1 mL of blood, previously drawn from the animal, with appropriate amounts of a 10 mg/mL solution of PTX in ethanol and re-instilling this blood intravenously to the animal as a bolus. This particular way of administering PTX (in rat blood) was used to overcome solubility issues in aqueous solutions. All other animals were treated with IPEC using Taxol®. In one study, the Taxol® excipients only (without PTX) were administered via IPEC to 2 rats to control for any pharmacological effects induced by the excipients. Furthermore, 8 rats received a 0.024 mg/mL PTX IPEC treatment, whereas the majority of the rats ($n=71$) received a 0.24 mg/mL IPEC treatment. The majority of the rats treated with IPEC were treated for 45 min ($n=67$). However, to study the effect of treatment duration, 4, 7 and 3 rats were treated for 5 min, 15 min and 30 min, respectively.

An overview of all collected data is given in Table 1 of the Supplementary material section.

PKPD Modelling

During model building, a sequential approach was adopted where PD data were added after optimization of the structural PK model. Data fitting was performed using the FOCE algorithm with interaction in NONMEM® (Version 7.2; Icon Development Solutions, Ellicott City, MD, USA). Prior to inclusion into the dataset, concentration measurements were log-transformed, whereas apoptosis measurements and tumour volume measurements were handled on the non-transformed scale. Inter-individual variabilities in PK parameters were modelled on the exponential scale whereas residual variability in the PK and PD data was modelled with, respectively, additive or proportional error structures. During model building PsN [8] and Pirana [9] were used as back- and/or front-end to NONMEM®. Graphical output from the model

as well as goodness-of-fit (GOF) plots that were used to guide model building were generated using Xpose (10).

Simulations

Simulations based on the final parameter estimates obtained from the PKPD model were performed in R®(R Foundation for Statistical Computing, Vienna, Austria) using user-written scripts based on a.o. the R-library deSolve (11). Throughout the simulation study, the effect of treatment was visualized for a tumour with a radius of 4 mm. Simulated endpoints include tumour PK and tumour apoptosis at 2 mm from the tumour surface and tumour growth curves after IPEC treatment. Furthermore, the R®-library PK (12) was used to calculate the area-under-the-curve (AUC) for the different simulated dosing schemes.

RESULTS

Exploratory Data Analysis of Tumour Tissue Concentrations

Prior to simultaneously modelling the PK of PTX in plasma and tumour after IPEC administration, we explored the PTX tumour concentration profiles separately. When plotting the ln-transformed PTX tumour concentrations as a function of depth from the tumour's dorsal surface, we noted a high degree of symmetry in the PTX concentrations on both sides of the tumour's centre. Therefore, in an attempt to evaluate whether differences exist in PTX penetration between the ventral or dorsal side of the tumour, we separated measurements based on their orientation relative to the tumour's centre prior to performing a simple linear regression analysis on both data sets.

Linear regression analysis, treating PTX concentration as the dependent and depth from tumour surface as the independent variable was performed using PROC REG in SAS® (SAS Institute Inc., Cary, NC, USA). When considering the standard errors associated with the estimated parameters, we found that neither the intercepts, nor the estimated slopes differed significantly. A GOF plot for the regression analysis is depicted in Fig. 2. This figure clearly shows that PTX penetrates the tumour equally efficient from both sides. Therefore, we decided, in the remainder of our PKPD analysis, to assume complete symmetry in PTX penetration in the tumour, irrespective of side.

Structural Pharmacokinetic Model

The pharmacokinetic model for PTX after IPEC is shown in Fig. 3; final parameter estimates are provided in Table I. The

system of differential equations that describe PTX disposition after IPEC is provided in the "Supplementary material".

PTX disposition after intravenous administration was best described by a 2-compartment model with first-order elimination from the central compartment (compartment 3 in Fig. 3). After fitting the 2-compartment model to the i.v. data alone, we decided, in order to increase model stability, to fix the parameters (Q, V_4) describing the peripheral distribution of PTX to their estimated values. It is worth noting that parameter estimates derived from our model are significantly higher than those reported by Jiko *et al.* (13) and Choi *et al.* (14). For example, we estimated plasma clearance to be 935 ($\pm$196) mL/h as compared to 323 mL/h and 321 mL/h found by Jiko *et al.* (13) and Choit *et al.* (14), respectively. Similar differences are noted for the other parameters (V_3, V_4, Q). However, this discrepancy is most probably explained by the fact that the excipients in Taxol® influence the PK of PTX after i.v. administration (15) and that in this part of our study, as opposed to Jiko *et al.* and Choi *et al.*, PTX was administered in its pure form (as described in the "Materials and Methods" section) rather than as Taxol® formulation.

Additional modifications to the i.v. model were made to account for the PK behaviour of PTX post IPEC administration. The structure of the model, with a parallel absorption into the plasma-, the tumour- as well as the depot compartment provides an adequate fit of the complex absorption pattern that is observed (GOF plots for individual predictions for both administered IPEC doses as well as the i.v. bolus dose are depicted in Fig. 4). The absorption from the peritoneal cavity (depicted by the dose compartment in Fig. 3) into the plasma compartment ($Zero_{13}$) is characterized by a zero-order process, inducing a rapid rise in plasma PTX concentrations after start of the IPEC administration. Simultaneously, a first-order, concentration-dependent absorption into plasma, through the depot compartment (characterized by rate constants k_{12} and k_{23}), further increases the uptake of PTX into plasma during IPEC administration. At the end of the procedure, when the peritoneal cavity is flushed and the rat's abdominal wall is sutured, this absorption route, from the depot compartment into plasma, adequately predicts the slow decrease or increase in plasma PTX concentrations post IPEC administration for the 0.024 and the 0.24 mg/mL perfusion concentrations respectively (Figure 1 in Supplementary materials). This depot compartment is thought to represent the lymphatic system draining the abdominal cavity, where PTX has specifically accumulated, e.g. in fat. As postulated by Lu *et al.* (16), absorption into the lymphatic system is one of the major processes responsible for clearing highly lipophilic compounds from the peritoneal cavity.

The absorption of PTX into the tumour was best characterized by a zero-order absorption process ($Zero_{15}$). Attempts to model tumour absorption using first-order processes or more complex non-linear absorption models consistently

Fig. 2 Goodness-of-fit plot for the linear regression analysis of PTX tumour concentrations. *Open circles* represent measured PTX tumour concentrations. The *solid lines* along with the dashed lines represent model predicted mean concentrations and the 95% confidence interval for the mean predicted tumour concentrations.
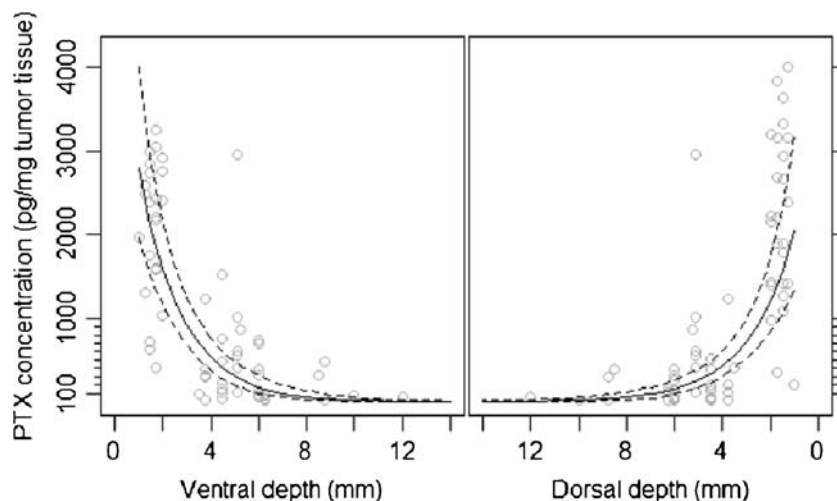
resulted in higher objective function values and worse GOF plots. This result is in agreement with earlier reports of saturable drug uptake by monolayer cultures of human cancer cells (17). A consequence of this saturable tumour absorption is that when administering PTX in high perfusate concentrations, several fold higher than the maximum uptake capacity of the tumour, changes in the perfusate concentrations will have little or no effect on the achieved tumour concentrations. This phenomenon is clearly illustrated in the GOF plot (Fig. 4), where for both administered IPEC doses, similar tumour concentrations were observed.

Despite the prolonged absorption from the peritoneal cavity into plasma, even after cessation of IPEC administration, during model building it became clear that absorption into the tumour continued only until IPEC administration was stopped. Furthermore, addition of an absorption process describing PTX absorption from plasma into tumour did not improve our model's performance. This is in line with earlier work by Lu *et al.* (18), who describes that following i.p. administration, plasma-to-tumour absorption is only a minor route of drug delivery to the tumour due to the relatively low drug concentration in blood.

Fig. 3 Overview of the structure of the final PK-PD model. The *black arrow* indicates the dosing compartment. Observations were recorded in compartments 1, 3, 5, 9 and 10.
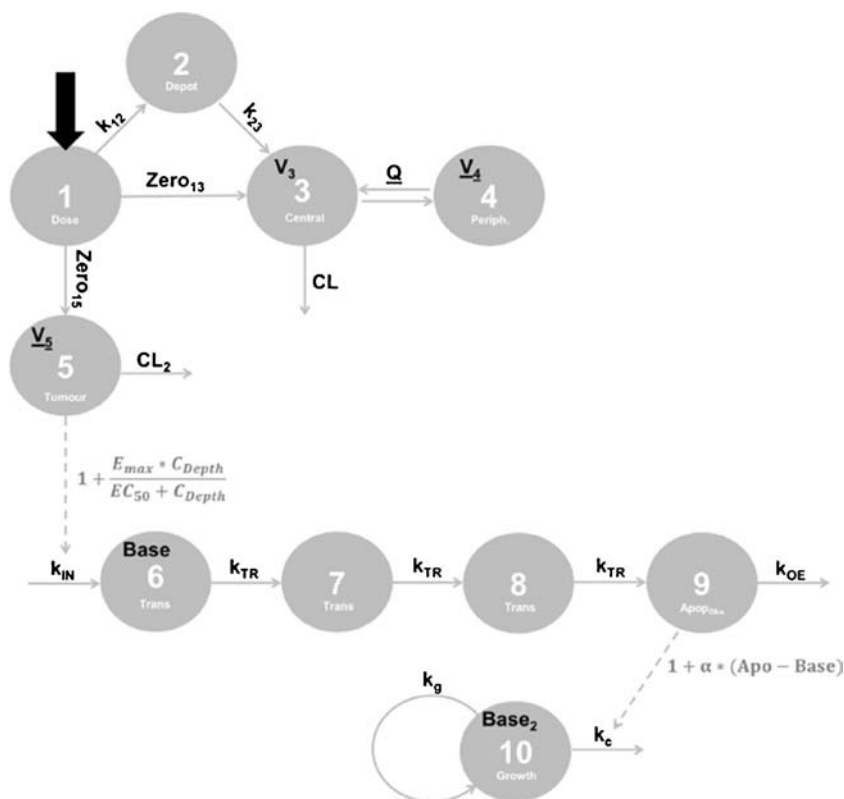
Table I Final Model Parameters as Well as Model Predicted Relative Standard Errors (RSE). The Parameter Estimates where the RSE is Missing are Parameters that were Fixed, i.e. these were not Estimated in the Final PKPD Model

Parameter	Estimate	RSE (%)
PK model		
K_{12}	0.393 h^{-1}	33.0
K_{23}	0.032 h^{-1}	35.0
$Zero_{13}$	$180\,\mu g \times h^{-1}$	27.0
V_3	2040 mL	26.0
CL_{Plasma}	$935\,mL \times h^{-1}$	21.0
V_4	2150 mL	–
Q	$1250\,mL \times h^{-1}$	–
$Zero_{15}$	$0.337\,\mu g \times h^{-1}$	21.0
V_5	0.025 g	–
CL_{Tumor}	0.0070 $g \times h^{-1}$	29.0
Slope	$-0.505\,\mu g \times (g \times mm)^{-1}$	14.0
Apoptosis model		
$Base_{Apoptosis}$	1.27%	5.0
E_{max}	19.8 h^{-1}	14.0
EC_{50}	$0.081\mu g \times g^{-1}$	49.0
MTT	0.845 h	19.0
k_{eo}	0.070 h^{-1}	10.0
Tumor growth delay model		
k_e	0.00010 h^{-1}	4.0
k_g	0.00230 h^{-1}	5.0
α	16.8 $(h \times \%\ apoptosis)^{-1}$	8.0
Inter individual variability		
	Estimate (CV %)	RSE (%)
W_{Zero13}	24.8	17.0
W_{Zero15}	10.2	23.0
W_{Slope}	4.1	19.0
Residual error model		
σ_{Comp1} (additive)	0.024	24.0
σ_{Comp3} (additive)	0.148	13.0
σ_{Comp5} (additive)	0.796	10.0
σ_{Comp9} (proportional)	0.276	7.0
σ_{Comp10} (proportional)	0.265	18.0

During model building it was decided to fix tumour volume (V_5) to 25 mg, the weight of the tumour sections that were used to quantify PTX tumour tissue concentrations. Fixing the tumour volume (V_5) provided the additional benefit of reducing the observed correlation between different parameters associated with the tumour compartment (CL_{Tumour}, slope, V_5), thereby providing stability to the model. Based on the model-estimated parameters, the half-life for PTX clearance from the tumour tissue was estimated to be approximately 2.5 h. This finding is different from the tumour tissue half-life of PTX as estimated from data reported by Desai *et al.* (19) (approximately 9 h). This difference is most likely

explained by the fact that Desai *et al.* (19) determined PTX concentrations in tumour homogenates, whereas we took the spatial distribution of PTX within solid tumours into account. Finally, from our model based slope estimate (-0.505 ± 0.071), we calculated that the "half-width" for PTX penetration is approximately 1.37 mm, i.e. PTX tumour concentrations reduce by half every 1.37 mm.

PKPD Model

As a starting point to link tumour concentrations to the observed apoptosis measurements, we used an adaptation of the transduction model as described by Gabrielsson and Weiner (20). Owing to the specific nature of the collected data, the typical system of differential equations used to describe the apoptosis as a function of time was modified to account for the depth at which the apoptosis measurements were performed (Details are provided in the "Supplementary material").

Using this transduction model, we estimated a.o. the time delay, expressed as mean transit time (MTT) between PTX binding to its intracellular receptor and the onset of the apoptosis to be 0.84 ($\pm$0.16) hours. Furthermore, our model estimates that the maximum apoptosis occurs approximately 14 h post IPEC treatment (Figure 2 in Supplementary material). By using this model, we assume that, within the tumours, a homeostasis exists between the onset (k_{in}) and the disappearance (k_{oe}) of apoptotic signals. In the absence of PTX, our model estimates that this homeostasis leads to a baseline apoptotic signal of 1.27 ($\pm$0.06) %. When PTX is present within tumours, it will stimulate the onset (k_{in}) of apoptotic signals, giving rise to an increase in observed apoptosis. PTX-induced changes in k_{in} were assumed to be additive and the concentration-effect relationship was modelled using an E_{max} model. From Table I it is noted that the EC_{50}, i.e. the tumour concentration at which half of the maximum effect is achieved, is 0.081 ($\pm$0.040) µg/g and that the maximum effect is 19.8 ($\pm$2.8), the latter amounting to an approximate 20-fold increase in k_{in}.

Finally, in an attempt to integrate information on tumour growth with the potential tumour growth inhibition of PTX, we explored the PDPD link suggested by Ait-Oudhia *et al.* (21). In their model describing a.o. PTX PKPD after i.v. administration of Taxol®, they assumed that the cytotoxicity induced by PTX is related to the kinetics and magnitude of the predicted apoptotic response. Based on this idea, we developed the final part of our model, assuming that tumour growth is governed by a balance between cell maturation/proliferation (k_g) on the one hand and cell death (k_e) on the other. In addition, it was assumed that by inducing apoptosis, cell death is stimulated. To produce predictions of tumour growth delay, we arbitrarily used predicted PTX-induced apoptosis at a depth half the size of the tumour radius as a

Fig. 4 Observed *versus* model predicted (IPRED) plasma (top left panel) and tumour concentrations (top right panel) as well as observed and model predicted apoptosis (bottom left panel) and tumour volume (bottom right panel) measurements.
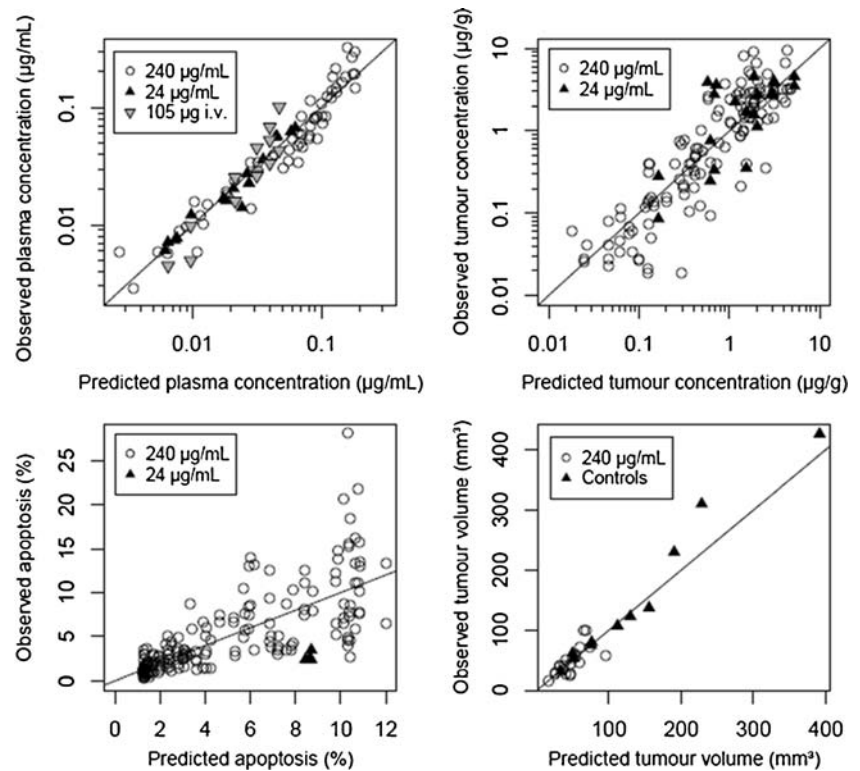
predictor. Therefore, the estimate α, is interpreted as the percentage increase in cell death rate (k_e) that is induced by achieving a 1% increase in apoptosis from baseline at a depth from the surface of ¼ the size of the tumour. In contrast to Ait-Oudhia *et al*. (21), we did take the spatial distribution of apoptosis within a solid tumour into account. Therefore, in the future, our model might serve as a tool for the comparison of treatment efficiencies for tumours of different size.

In the absence of PTX, our model adequately captures the growth of the tumours as observed from the control group (Fig. 4). Moreover, when PTX is administered via IPEC, as seen in Figure 2 of the Supplementary materials, our predictions adequately capture the biphasic evolution of tumour volume post-dosing. It is predicted that prior to regrowth, tumour volume reaches a minimum approximately 50 h post dose.

PKPD Simulations

To evaluate the effect of changing perfusate concentrations or treatment duration on the outcome of the IPEC procedure, several treatment modalities were simulated. Using our final model parameter estimates, we simulated 15, 45, 90 and 120 min IPEC administrations at concentrations ranging between 0.01 µg/mL and 100 µg/mL. Typical tumour and plasma exposure (AUC obtained using non-compartmental

analysis of simulated concentrations) for the different simulated IPEC treatments are depicted in Fig. 5.

From our simulations, it can be seen that $\text{AUC}_{\text{Tumour}}$ reaches a maximum at a particular perfusate concentration. Increasing the perfusate concentration beyond this point does not increase $\text{AUC}_{\text{Tumour}}$ any further. In addition, the perfusate concentration producing maximum tumour exposure depends on the treatment duration. For the 15, 45, 90 and 120 min treatment durations, our simulations show that perfusate concentrations attaining maximum tumour exposure are 0.40, 1.60, 4.00 and 6.35 µg/mL respectively. The achieved maximum $\text{AUC}_{\text{Tumour}}$ differs significantly between the simulated treatments. The maximum $\text{AUC}_{\text{Tumour}}$ is 4.30, 13.09, 26.24 and 35.00 µg.h/g for the 15, 45, 90 and 120 min treatments, respectively.

When evaluating $\text{AUC}_{\text{Plasma}}$, our simulations show that no such maximum exposure is achieved in plasma. For every simulated treatment, a clear positive correlation is observed between perfusate concentrations and $\text{AUC}_{\text{Plasma}}$. A useful therapeutic index, weighing the desirable effect of the treatment (high $\text{AUC}_{\text{Tumour}}$) by the unwanted effects of the treatment (high $\text{AUC}_{\text{Plasma}}$, hence high probability of systemic toxicities) is the $\text{AUC}_{\text{Tumour}}$ over $\text{AUC}_{\text{Plasma}}$ ratio. When evaluating this index for the different simulated treatments, it can be seen that this index, depicted by the continuous line in Fig. 5, is high up to the perfusate concentration that achieves maximum tumour exposure. Beyond this point, this

Fig. 5 AUC$_{Tumour}$ and AUC$_{Plasma}$ as a function of treatment duration (15, 45, 90 and 120 min treatments in the top-left, top-right, bottom-left and bottom-right panels, respectively) and perfusate concentration. The *shaded grey area* depicts the AUC$_{Plasma}$, whereas the *solid line with embedded symbols* depicts the AUC$_{Tumour}$. The *solid line* represents the AUC$_{Tumour}$ over AUC$_{Plasma}$ ratio and its values are plotted against the left y-axis. The *dashed lines* represent the coordinates of the "saturation point".
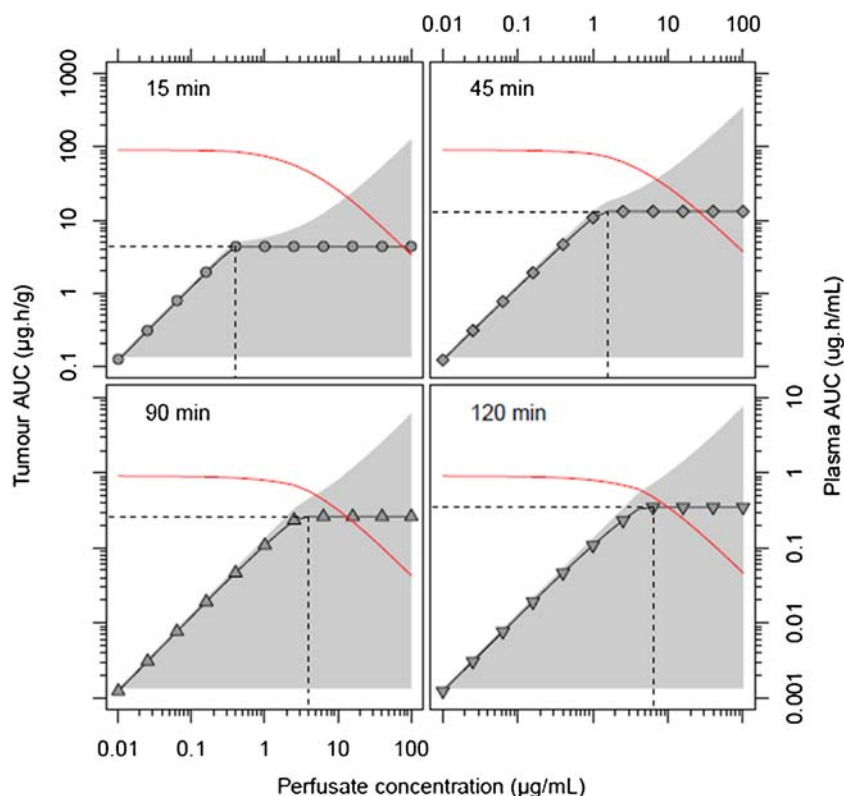
index declines steeply, indicating a less efficient delivery of PTX to its site of action.

To compare the different simulated treatments at their optimal perfusate concentration (the lowest perfusate concentration achieving maximum AUC$_{Tumour}$), additional simulations were performed. Figure 6 shows the plasma-concentration-time profile as well as the evolution of the tumour volume following IPEC administration for the different optimal treatment duration/perfusate concentration combinations.

From Fig. 6 it can be seen that peak plasma concentrations differ 4-fold between the shortest and the longest treatment duration. This difference in plasma concentrations is reflected in the overall plasma exposure (AUC$_{Plasma}$ for the different simulated treatments is 0.05, 0.18, 0.46 and 0.72 µg.h/mL, respectively). Of note is that AUC$_{Tumour}$ (cfr. supra) differs approximately 8-fold, whereas AUC$_{Plasma}$ differs approximately 14-fold between the shortest and the longest treatment duration. When comparing the different treatments in terms of the AUC$_{Tumour}$ over AUC$_{Plasma}$ ratios, we found that the index decreases from approximately 85 for the 15 min treatment until 49 for the 120 min treatment.

The lower panel of Fig. 6 shows the evolution of tumour volume following the different treatments. Although none of the treatments achieves a complete reduction of the tumour, significant differences are observed between the simulated treatments. The achieved tumour shrinkage at approximately

50 h post treatment is 25, 35, 42 and 45% for the 15, 45, 90 and 120 min treatment durations, respectively.

DISCUSSION

Based on our elaborate tumour tissue sectioning protocol we showed, in contrast to our expectations, that in our rat model, tumours attached to the peritoneal membrane are equally accessible for drug penetration from the ventral as well as the dorsal side. This finding is somewhat counterintuitive because of the perceived restricted access of the cytotoxic solution towards the ventral part of the tumour, which is attached to the peritoneal membrane. One plausible explanation might be that, the barrier between the cytotoxic solution in the peritoneal cavity and plasma, i.e. the peritoneum, does not correspond to the classic semipermeable membrane. Rather than being a physical transport barrier, its complex structure makes it highly permeable to water, small solutes and proteins (22), thereby potentially allowing peritoneal tumours to be homogeneously exposed to the cytotoxic solution. Another explanation for this peculiar finding might be that the tumours in our animal model, which are artificially grown on the peritoneum, might be somewhat more accessible to drugs than tumours that naturally occur in PC. However, given the lack of other studies that quantitatively evaluated tumour

Fig. 6 Model predicted time-course of PTX plasma concentrations and tumour volume post IPEC dosing.
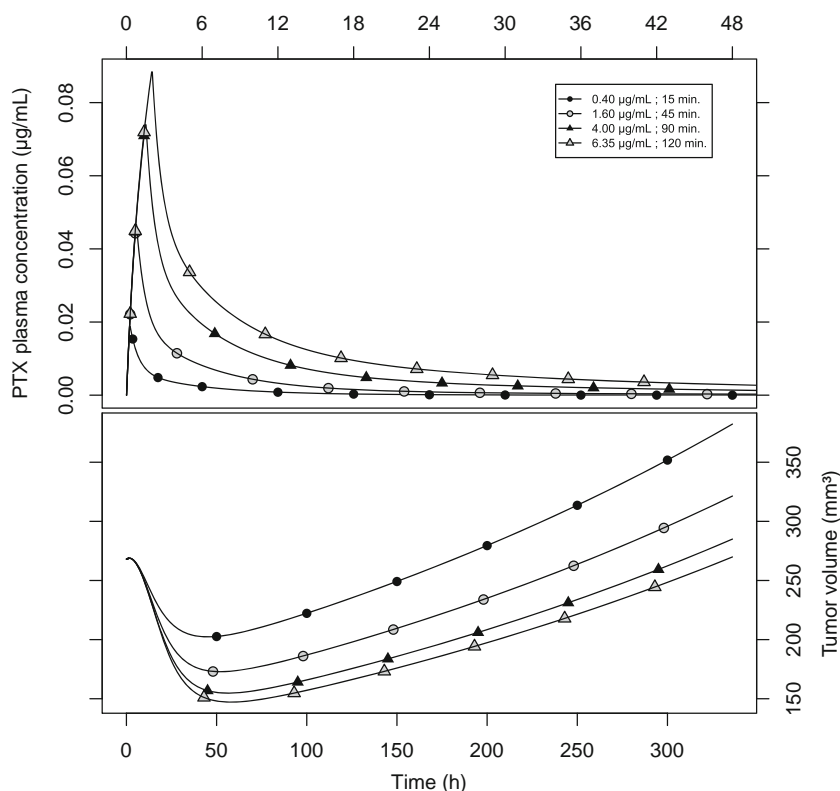
penetration post IPEC dosing, these hypotheses remain to be confirmed.

When comparing the extent of PTX tumour penetration that was observed in our study (half-width approximately 1.37 mm) against earlier reports (23–27), it stands out that the extent and the kinetics of tumour penetration of PTX are significantly different in our study. Overall, *in-vitro* studies using a.o. multicellular layer cultures, show that PTX penetrates only a few cell layers (approximately 100 μm). Even in *in-vivo* models of i.p. administration of PTX nano-/microparticles, used by Kamei *et al.* (24) and Lu *et al.* (28), penetration was limited to approximately 1 mm. Not only does the extent of tumour penetration in our study widely differ from these earlier reports (Fig. 2 shows that post IPEC PTX was measured even at 12 mm from the tumour's surface), the kinetics of penetration are different as well.

Earlier studies (23–28) showed that PTX penetration is slow, whereas we found that even at 15 min post IPEC administration, significant PTX tumour concentrations (>0.035 μg/g) are detected in the tumour's centre. Although these different kinetics might be attributed to the experimental design (most literature reports originate from *in-vitro* studies), the specific nature of the IPEC administration could be responsible for this phenomenon. On the one hand, the superior distribution of the perfusate within the abdominal cavity as opposed to the classical i.p. injection, bringing the cytotoxic solution in close contact with the tumour's surface might be responsible for the faster tumour penetration. On the other

hand, owing to the fact that drug penetration in solid tumours is governed by passive diffusion as well as convective processes (28), the hydrostatic pressure induced by the cytotoxic solution within the abdominal cavity might enhance convection towards the tumour's interstitium, thereby increasing tumour penetration. Future work should be directed towards unravelling the physical/chemical phenomena that explain the higher degree of PTX tumour penetration following IPEC as compared to other routes of administration.

The results from our simulation study show that, in our animal model, even optimized combinations of treatment duration and perfusate concentration will not produce full tumour shrinkage after a single IPEC administration of PTX. Multiple dose strategies seem to be necessary to induce complete tumour shrinkage after IPEC treatment. On the other hand, our simulations also show that increasing treatment duration, whilst concurrently increasing the perfusate concentration, holds additional benefits in terms of achieving higher tumour exposure. This finding is in agreement with other reports on i.p. PTX dosing in the literature (27,28), that describe that in order to optimize pharmacological response, exposure to the cytotoxic agent should be prolonged. Our model, which simultaneously describes plasma- as well as tumour exposure after IPEC administration of PTX could be used to determine the characteristics of a modified release formulation producing maximal tumour exposure whilst simultaneously minimizing systemic exposure.

CONCLUSIONS

Based on our animal studies, we clearly identified a non-linear dose–response relationship originating from saturable absorption into the tumour. Furthermore, we showed that IPEC treatment modalities differently affect tumour and plasma exposure, thereby allowing the optimisation of the therapeutic range, i.e. separating treatment efficiency from possible systemic toxicities. The complex processes underlying the absorption from PTX from the peritoneal cavity after IPEC and the interplay of these processes on efficacy and potential systemic toxicities make that for PTX dosing via IPEC less might truly result in more.

We hypothesize that, based on the close resemblance between tumour exposure in our animal model and tumour exposure in patients treated under similar conditions, our study results are of great value for all stakeholders involved in the development of new treatment protocols for PC using IPEC.

ACKNOWLEDGMENTS AND DISCLOSURES

REFERENCES

1. Spratt JS, Adcock RA, Muskovin M, Sherrill W, Mckeown J. Clinical delivery system for intra-peritoneal hyperthermic chemotherapy. Cancer Res. 1980;40(2):256–60.

2. Cascales PA, Gil J, Galindo PJ, Machado F, Frutos IMM, Paricio PP. Heterogeneity in patients and methods. A problem for hyperthermic intraoperative intraperitoneal chemotherapy (HIPEC) in ovarian carcinoma. Eur J Obstet Gynecol Reprod Biol. 2011;158(2):361–2.

3. Dedrick RL, Flessner MF. Pharmacokinetic problems in peritoneal drug administration: tissue penetration and surface exposure. J Natl Cancer Inst. 1997;89(7):480–7.

4. Hasovits C, Clarke S. Pharmacokinetics and pharmacodynamics of intraperitoneal cancer chemotherapeutics. Clin Pharmacokinet. 2012;51(4):203–24.

5. Van Der Speeten K. A pharmacokinetic and pharmacodynamic rationale for perioperative cancer chemotherapy in patients with peritoneal carcinomatosis. Uppsala University; 2010.

6. De Smet L, Colin P, Ceelen W, Bracke M, Van Bocxlaer J, Remon JP, *et al*. Development of a nanocrystalline paclitaxel formulation for hipec treatment. Pharm Res. 2012;29(9):2398–406.

7. Guideline on bioanalytical method validation. Guideline on bioanalytical method validation. European Medicines Agency 2012 Feb 1.

8. Lindbom L, Ribbing J, Jonsson EN. Perls-speaks-NONMEM (PsN)—a Perl module for NONMEM related programming. Comput Methods Prog Biomed. 2004;75(2):85–94.

9. Keizer RJ, van Benten M, Beijnen JH, Schellens JHM, Huitema ADR. Pirana and PCluster: a modeling environment and cluster infrastructure for NONMEM. Comput Methods Prog Biomed. 2011;101(1):72–9.

10. Jonsson EN, Karlsson MO. Xpose—an S-PLUS based population pharmacokinetic/pharmacodynamic model building aid for NONMEM. Comput Methods Prog Biomed. 1999;58(1):51–64.

11. Soetaert K, Petzoldt T, Setzer RW. Solving differential equations in R: package deSolve. J Stat Softw. 2010;33(9).

12. Jaki T, Wolfsegger MJ. Estimation of pharmacokinetic parameters with the R package PK. Pharm Stat. 2011;10(3):284–8.

13. Jiko M, Yano I, Okuda M, Inui K. Altered pharmacokinetics of paclitaxel in experimental hepatic or renal failure. Pharm Res. 2005;22(2):228–34.

14. Choi BC, Choi JS, Han HK. Altered pharmacokinetics of paclitaxel by the concomitant use of morin in rats. Int J Pharm. 2006;323(1–2): 81–5.

15. Sparreboom A, van Tellingen O, Nooijen WJ, Beijnen JH. Nonlinear pharmacokinetics of paclitaxel in mice results from the pharmaceutical vehicle Cremophor EL. Cancer Res. 1996;56(9): 2112–5.

16. Lu Z, Wang J, Wientjes MG, Au JLS. Intraperitoneal therapy for peritoneal cancer. Future Oncol. 2010;6(10):1625–41.

17. Kuh HJ, Jang SH, Wientjes MG, Weaver JR, Au JLS. Determinants of paclitaxel penetration and accumulation in human solid tumor. J Pharmacol Exp Ther. 1999;290(2):871–80.

18. Lu D, Wientjes MG, Lu Z, Au JLS. Tumor priming enhances delivery and efficacy of nanomedicines. J Pharmacol Exp Ther. 2007;322(1):80–8.

19. Desai N, Trieu V, Yao ZW, Louie L, Ci S, Yang A, *et al*. Increased antitumor activity, intratumor paclitaxel concentrations, and endothelial cell transport of Cremophor-free, albumin-bound paclitaxel, ABI-007, compared with Cremophor-based paclitaxel. Clin Cancer Res. 2006;12(4):1317–24.

20. Gabrielsson G, Weiner D. Pharmacokinetic and pharmacodynamic data analysis: concepts and applications. 4th edition ed. 2007.

21. Ait-Oudhia S, Straubinger RM, Mager DE. Systems pharmacological analysis of paclitaxel-mediated tumor priming that enhances nanocarrier deposition and efficacy. J Pharmacol Exp Ther. 2013;344(1):103–12.

22. Flessner MF. The transport barrier in intraperitoneal therapy. Am J Physiol Ren Physiol. 2005;288(3):F433–42.

23. Jang SH, Wientjes MG, Au JLS. Determinants of paclitaxel uptake, accumulation and retention in solid tumors. Investig New Drugs. 2001;19(2):113–23.

24. Kamei T, Kitayama J, Yamaguchi H, Soma D, Emoto S, Konno T, *et al*. Spatial distribution of intraperitoneally administered paclitaxel nanoparticles solubilized with poly (2-methacryloxyethyl phosphorylcholine-co n-butyl methacrylate) in peritoneal metastatic nodules. Cancer Sci. 2011;102(1):200–5.

25. Kyle AH, Huxham LA, Yeoman DM, Minchinton AI. Limited tissue penetration of taxanes: a mechanism for resistance in solid tumors. Clin Cancer Res. 2007;13(9):2804–10.

26. Lee JH, Na K, Song SC, Lee J, Kuh HJ. The distribution and retention of paclitaxel and doxorubicin in multicellular layer cultures. Oncol Rep. 2012;27(4):995–1002.

27. Nicholson KM, Bibby MC, Phillips RM. Influence of drug exposure parameters on the activity of paclitaxel in multicellular spheroids. Eur J Cancer. 1997;33(8):1291–8.

28. Lu Z, Tsai M, Lu D, Wang J, Wientjes MG, Au JLS. Tumor-penetrating microparticles for intraperitoneal therapy of ovarian cancer. J Pharmacol Exp Ther. 2008;327(3):673–82.